Iranian Journal of Materials Forming 11 (3) (2024) 28-39

Online ISSN: 2383-0042

IJMF

Iranian Journal of Materials Forming

Journal Homepage: http://ijmf.shirazu.ac.ir

Research Article

Investigation of Post-Buckling, Energy Harvesting, and Relaxation of Shape Memory Auxetic Structure with Thermo-Visco-Hyperelastic Modeling

S. Vaziri and K. Narooei*

Department of Materials Science and Engineering, K. N. Toosi University of Technology, Tehran, Iran

ARTICLE INFO

Article history:

Received 25 August 2024
Reviewed 9 November 2024
Revised 9 December 2024
Accepted 10 December 2024

Keywords:

Auxetic structure
Shape memory polymers
Thermo-hyper-viscoelastic
Buckling
Pattern transformation

Please cite this article as:

Vaziri, S., & Narooei, K. (2024). Investigation of post-buckling, energy harvesting, and relaxation of shape memory auxetic structure with thermo-visco-hyperelastic modeling. *Iranian Journal of Materials Forming*, *11*(3), 28-39. https://doi.org/10.22099/ijmf.2024.51080.1302

ABSTRACT

This study investigated the non-linear post-buckling behavior of an auxetic cellular structure under compressive loading, with variations in temperature and strain rate. Simulations were conducted on epoxy shape memory polymer (SMP) incorporating different geometrical imperfections derived from buckling analysis. A hyper-viscoelastic model, coupled with the Williams-Landel-Ferry (WLF) equation, was employed, enabling thermo-hyper-viscoelastic modeling that accounts for temperature dependency. The results demonstrated that the imperfection factor significantly changes the shape transformation, and an imperfection factor of 0.01 was used for subsequent simulations. It was observed that increasing the temperature up to 50 °C increases the critical strain required for pattern transformation, while further temperature increases lead to a decrease in the critical strain. Additionally, increasing the strain rate from 0.01 /s to 1 /s raises the absorbed energy from 0.53 J/cm^3 to 1.72 J/cm^3 while increasing the temperature reduces the absorbed energy due to the rise in loss modulus. It was also found that, irrespective of strain rate variation, the Poisson's ratio remains around 0.4 and decreases to negative values as the deformation exceeds the critical strain.

1. Introduction

In recent years, auxetic structures have gained widespread applications in fields such as medicine, aerospace, and architecture. Their design methodology combines structural analysis with the mechanical behavior of materials. In addition to mechanical loadings, factors such as strain rate and temperature significantly influence Poisson's ratio of shape memory auxetic structures due to the local buckling of ligaments that leads to pattern transformation. Additionally, porosity plays a critical role in heat transfer [1], pattern transformation [2], and, subsequently, the shape memory behavior of auxetic structure [3]. Consequently,

* Corresponding author
E-mail address: knarooei@kntu.ac.ir (K. Narooei)
https://doi.org/10.22099/ijmf.2024.51080.1302

researchers have explored the effects of porosity shape and volume fraction on the mechanical behavior of auxetic materials [4, 5]. The findings revealed that the negative Poisson's ratio, a hallmark of auxetic behavior, is influenced by the shape and volume fraction of porosity [6, 7]. This behavior presents considerable importance across various engineering disciplines. For instance, certain muscles and tendons in athletes are prone to injury, and studies have shown that artificial tendons, designed with auxetic structures, can support tissue recovery [8]. Additionally, the challenge of powering sensors in inaccessible locations can be addressed by harnessing energy from deformation, where the combination of auxetic behavior and piezoelectric properties has been shown to enhance energy harvesting efficiency [9].

Buckling is a common phenomenon observed in members subjected to compressive loads [10]. Porous members often exhibit both Euler and alternate buckling modes as a result of pattern transformation. The Euler mode is characterized by buckling in a direction perpendicular to the axis of compression, while alternate modes involve the deformation of holes into horizontal and vertical ellipses, while the member remains approximately straight [11]. The transition between these modes, known as the switching or pattern transformation phenomenon, is induced by local elastic instabilities [12]. Numerical modeling of buckling behavior has shown that geometric imperfections are necessary to capture the bifurcation caused by buckling, typically represented as a geometrical perturbation by a fraction of the buckling modes [13, 14]. Different studies have employed different imperfection coefficients, generally around 0.1 of the buckling modes, depending on the case study [15]. Another critical factor influencing the time-dependent behavior of materials is the strain rate. In this regard, Su et al. [16], Li et al. [17], and Arman and Narooei [18] have investigated the mechanical behavior of materials under different loading rates. It has been observed that the buckling modes of bilayer beams with rate-dependent mechanical behavior (hyper-viscoelastic) are significantly affected by the loading rate [19]. Additionally, when shape memory polymers are used in constructing auxetic structures, temperature becomes a crucial factor influencing their behavior. Thermo-hyper-viscoelastic models, incorporating the Williams-Landel-Ferry (WLF) equation, are often employed to account for temperature effects on shape memory behavior [20].

Extensive research has explored the effects of cellular geometry and material properties on auxetic behavior. It has been observed that local instability (buckling) in the ligaments of auxetic structures leads to the appearance of a plateau in the stress-strain curve after reaching a critical strain threshold [21]. Beyond geometry, impact loading has been found to induce variable Poisson's ratios in auxetic structures [22], which may be linked to the rate-dependent behavior of the material [19]. Studies on holed structures made from silicone rubber have revealed variable Poisson's ratios with a mechanism involving rigid body rotation, resulting in both auxetic and non-auxetic behavior [23]. Compression of 2D structures and shells patterned with circular holes has shown that local buckling can be induced by tuning the porosity and shell thickness, transforming the initial microstructure into a mutually orthogonal ellipse [24, 25]. Studies on perforated hard materials have demonstrated that auxetic behavior can be achieved through pattern transformation rather than localized failure modes such as shear banding [26].

In this study, the auxetic behavior of shape memory epoxy specimens under uniaxial compression was investigated using numerical methods. The effects of loading rate (strain rate) and temperature on auxetic behavior were examined using a thermo-hyper-viscoelastic model. The literature review reveals a gap in considering imperfections in the buckling modes (local or global) of auxetic structures. To bridge this gap, a buckling analysis of circular-holed structures was conducted. Subsequently, the non-linear behavior of auxetic structures under compressive loads was investigated by subjecting samples with an imperfection magnitude of 0.01 of the buckling mode to various temperatures and strain rates. This study also aims to identify the stored energy of structure, particularly at temperatures above the glass transition temperature (T_g),

an area which has not been thoroughly explored in previous research. Section 2 provides details on the simulation of the pattern and the behavior of shape memory polymers, while section 3 examines the buckling of the samples and its effects, energy absorption, and Poisson's ratio of the auxetic structures.

2. Simulation

In this research, a periodic circular-hole plate with dimensions of 100×100×5 mm^3 and a porosity of 59% (corresponding to hole radii of 4.335 mm) was analyzed. The sample was meshed using 7089 linear hexahedral elements with a hybrid formulation (C3D8RH elements) to account for material incompressibility. This number of elements has been chosen to avoid the buckling mode shape and the element size. This structure represents the minimum porosity (critical porosity) necessary to initiate auxetic behavior; below this porosity threshold, the structure exhibits conventional (non-auxetic) behavior [3]. The mechanical behavior of the epoxy shape memory polymer (SMP) was modeled using a thermo-hyper-viscoelastic approach, as described in previous studies [27, 28]. The Prony series coefficients used for this polymer are provided in Table 1 [20]. These parameters were derived from the dynamic mechanical thermal analysis (DMTA) by fitting the storage and loss modulus to the Prony series. In this model, $g_i's$ and $\tau_i's$ represent the coefficients and relaxation times used to describe the viscoelastic response with the Prony series. The same material parameters were employed in reference [3], which served as a basis for the comparison with the simulation results.

The incompressible Neo-Hookean hyperelastic model was employed to simulate the elastic behavior of the material, with the corresponding coefficient C_{10}=393.96 MPa [20]. The effect of temperature on the shape memory behavior of the epoxy polymer was accounted using the Williams-Landel-Ferry (WLF) equation as described in [29, 30]:

$$Log(a_T) = \frac{-C_1(T - T_{ref})}{C_2 + T - T_{ref}} \quad (1)$$

Where $a_T(T)$ is the time-temperature superposition shifting factor, C_1 and C_2 are material constants, and T_{ref} is the reference temperature. The WLF parameters were considered as C_1=10.17, C_2=47.35 ℃, and, T_{ref}=50 ℃ [20].

All results were obtained through simulations conducted in ABAQUS software at various temperatures and strain rates. In all simulations, the bottom of the samples was constrained in both vertical and horizontal directions. Uniaxial compression was applied via a displacement control method, where the displacement was assigned to a reference point coupled to the top surface of the sample (Fig. 1).

Since a time-dependent constitutive model (thermo-hyper-viscoelastic) was employed in this research, the rate effect had to be incorporated into the applied boundary conditions. Table 2 presents the strain rate ranges corresponding to the applied velocity boundary conditions. To ensure consistent strain for all simulations, the duration of each simulation was adjusted according to the values listed in the last column of Table 2. Additionally, the relaxation behavior of the SMPs was simulated to investigate the underlying causes of Poisson's ratio variation. The specific conditions for these simulations are presented in Table 3.

In all simulations, the process began with a buckling analysis and subsequently, a compression (post-buckling) analysis was conducted using a second model. This post-buckling analysis was coupled with the initial buckling analysis to account for geometric imperfections.

Table 1. Prony series coefficients for the epoxy shape memory polymer [20]

$\tau_i(s)$	0.3031×10^{-4}	0.1721×10^{-3}	0.9768×10^{-3}	0.5545×10^{-2}	0.3147×10^{-1}	0.1787
$g_i(Pa)$	0.1476×10^{9}	0.1756×10^{9}	0.2025×10^{9}	0.1775×10^{9}	0.6802×10^{8}	0.1139×10^{8}
$\tau_i(s)$	0.1014×10^{1}	0.5757×10^{1}	0.3268×10^{2}	0.1855×10^{3}	0.1053×10^{4}	0.5977×10^{4}
$g_i(Pa)$	0.2264×10^{7}	0.8132×10^{6}	0.4020×10^{6}	0.1760×10^{6}	0.5056×10^{5}	0.1265×10^{5}

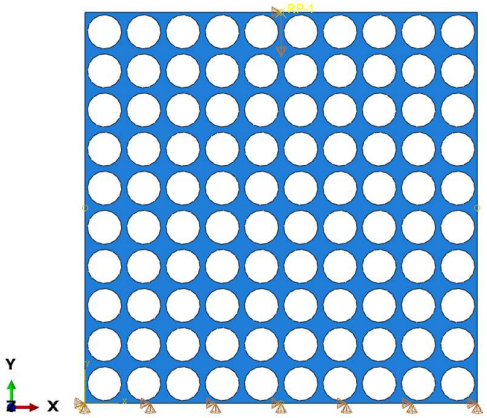

Fig. 1. Applied boundary condition of auxetic periodic circular pattern.

Table 2. Simulation conditions for post-buckling analysis

Strain rate (/s)	Applied velocity (mm/s)	Time (s)
0.01	1	10
0.1	10	1
1	100	0.1

Table 3. Simulation conditions for relaxation analysis

Loading time (s)	Relaxation time (s)	Temperature (°C)
0.1	50	40
0.1	50	50
0.1	50	60

3. Results and Discussion

In general, buckling in auxetic structures under compressive load can manifest as either Euler buckling or local buckling of ligaments. The Euler mode occurs when the sample buckles in a direction perpendicular to the compression axis. In contrast, alternating modes involve local buckling without global instability; for a circular-holed plate, the holes deformed into horizontal and vertical ellipses while the overall structure remains nearly straight [11]. To accurately investigate buckling behavior numerically, it is essential to introduce a geometric imperfection, typically related to the sample's thickness [13, 14]. The four deformation modes of circular-holed auxetic structures are illustrated in Fig. 2. It is important to note that these are the various deflected shapes a structure can assume after buckling, rather than actual deformations resulting from the applied load. Mathematically, buckling modes correspond to the eigenvalues and eigenvectors of the system's stiffness matrix, where the eigenvalues are linked to critical loads and the eigenvectors represent the mode shapes.

As shown in Fig. 2, the first four buckling modes demonstrate that local instability and pattern transformation can lead to auxetic deformation in the sample. A geometric imperfection pattern must be introduced into the perfect geometry to ensure that a post-buckling problem exhibits a continuous response instead of bifurcation. This approach allows for some deformation in the buckling mode even before the critical load is reached. In the post-buckling analysis, an imperfection factor of 0.01 of the modes shown in Fig. 2 was applied to analyze the non-linear behavior of the proposed auxetic structures. The stress-time response from the post-buckling analysis can be seen in Fig. 3.

In the first step, Fig. 3 presents a comparison between the current results and the simulations from reference [3] under the same boundary conditions. The observed discrepancies are attributed to the use of periodic boundary conditions and representative volume elements (RVE) in reference [3]. A comparison between the results of the current simulations and those obtained using RVE is shown in Fig. 4. The stress values in all subsequent figures are expressed in MPa. Figs. 4(a) to 4(c) illustrate the deformation of the auxetic structure corresponding to the first stress plateau (points I, II, and III in Fig. 3). By examining these figures, it can be understood by increasing the imperfection factor, the critical strain also increases as the local deformation of circular holes postpones the drop in the load that indicates the first appearance of buckling. Fig. 4(d) shows that despite the variation in imperfection factors, all structures ultimately reach a similar final deformation, leading to the same final stress plateau observed in Fig. 3. A comparison between Figs. 4(d) and 4(e) reveals that using symmetry or periodic boundary conditions on an RVE cannot accurately predict the exact deformation pattern of the full sample. Imposing periodic boundary conditions (as done in reference [3]) imposes the homogenous deformation due to the constraint of the left and right boundaries to the same deformation as shown in Fig. 4(e). However, as seen in Fig. 4(d), when the full sample is loaded, the free left and right boundaries produce non-homogenous deformation.

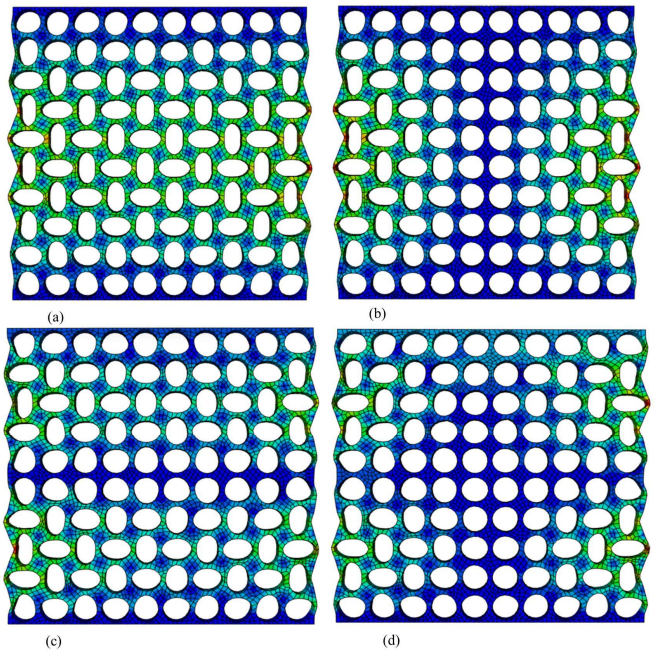

Fig. 2. Buckling modes of auxetic circular-hole structure: (a) mode I, (b) mode II, (c) mode III, and (d) mode IV.

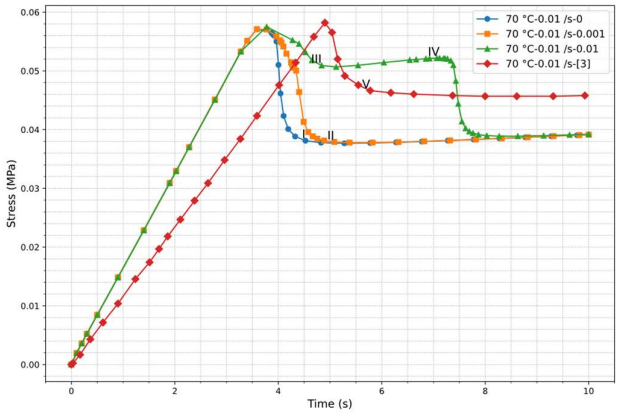

Fig. 3. Stress-time curves for different imperfection factors at 70 °C, compared with the simulations from [3].

This discrepancy explains the differences between the simulation results in Fig. 3 of the current study, which does not include imperfection, and the RVE simulations in reference [3].

Fig. 3 illustrates that at the onset of the first buckling event, all structures exhibit a similar maximum load, leading to a comparable deformation at this stage. Figs. 5(a) through 5(c) present the deformed structures corresponding to the maximum load depicted in Fig. 3. As observed, the deformed geometries show no significant differences, as anticipated. Therefore, it can be inferred that while the imperfection factor significantly influences the post-buckling behavior, it does not have a notable impact on the initial buckling characteristics of circular-holed auxetic structures.

As the behavior of shape memory materials depends on temperature and strain rate, compressive loading simulations were conducted at temperatures of 40, 50, and 60 °C, with strain rates of 0.01, 0.1, and 1 /s. The predicted stress-strain responses under these conditions are presented in Fig. 6.

A comparison of Figs. 6(a) to 6(c) reveals that the material exhibits a stiffer response with an increase in strain rate, while higher temperatures result in significant softening. To illustrate the pattern transformation during deformation, the deformed geometries at points I, II, and III in Fig. 6 (a) are shown in Fig. 7. From Fig. 7, it is evident that the first local buckling occurs at point I in

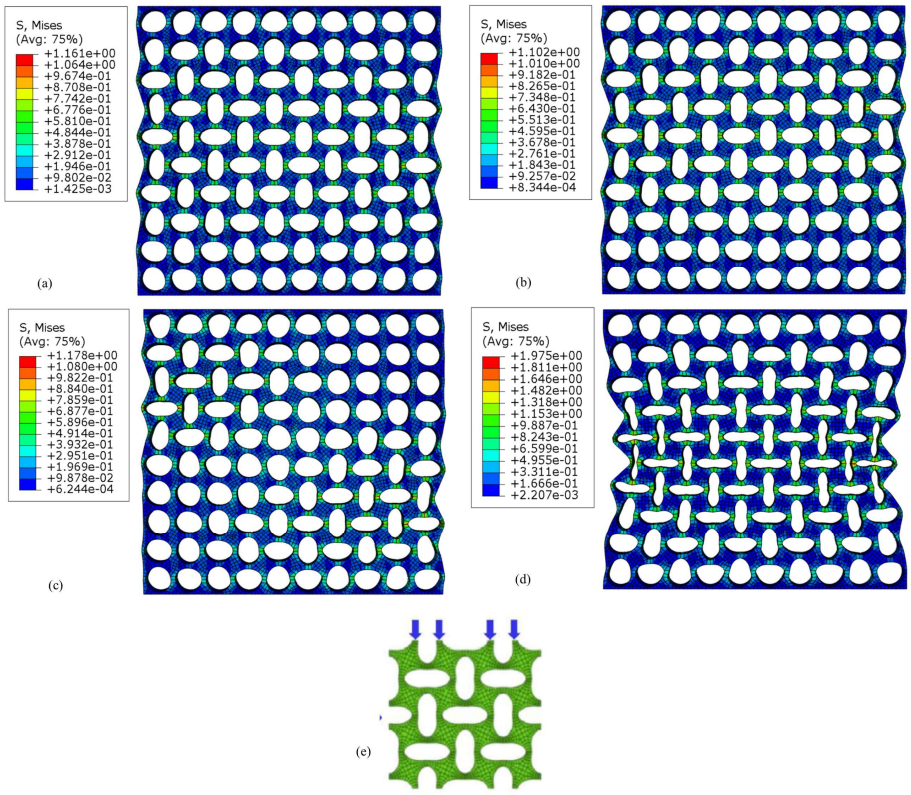

Fig. 4. Post-buckling analysis of holed auxetic structure at 70 °C and a strain rate of 0.01 /s: (a) without imperfection at I, (b) imperfection of 0.001 at mode II, (c) imperfection of 0.01 at mode III, (d) final deformation of all structures, and (e) RVE simulations from reference [3].

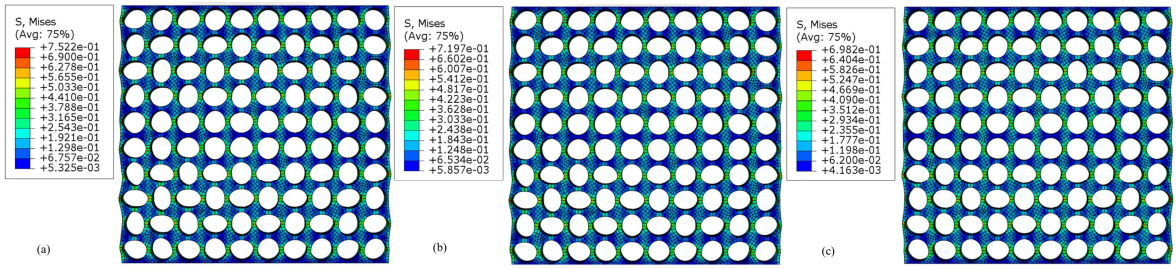

Fig. 5. Deformed geometry at maximum load in Fig. 3, at 70 °C and strain rate of 0.01 /s: (a) without imperfection, (b) imperfection of 0.001, and (c) imperfection of 0.01.

Fig. 6 (a), while pattern transformation takes place at point II. At point III, fully developed local buckling and auxetic behavior are expected. Similar observations can be made for other strain rates and temperatures depicted in Fig. 6.

By carefully examining the critical strain (the strain at maximum load), it becomes evident that the critical strain is a function of both strain rate and temperature. The critical strain values for each temperature and strain rate were extracted and plotted in Fig. 8. The plot shows that the critical strain increases with temperature up to 50 °C and then decreases, consistent with the results reported by He et al. [3]. However, it is important to note that while a similar trend is observed in [3], the critical strain values differ in this study due to the use of periodic boundary conditions on the representative volume element (RVE) in He et al.'s work. As previously mentioned, this assumption fails to capture the full deformation of the sample. In the post-buckling analysis, since the samples exhibit non-homogeneous deformation (Fig. 4), the predictions based on RVE cannot accurately reflect the exact deformation behavior of the samples.

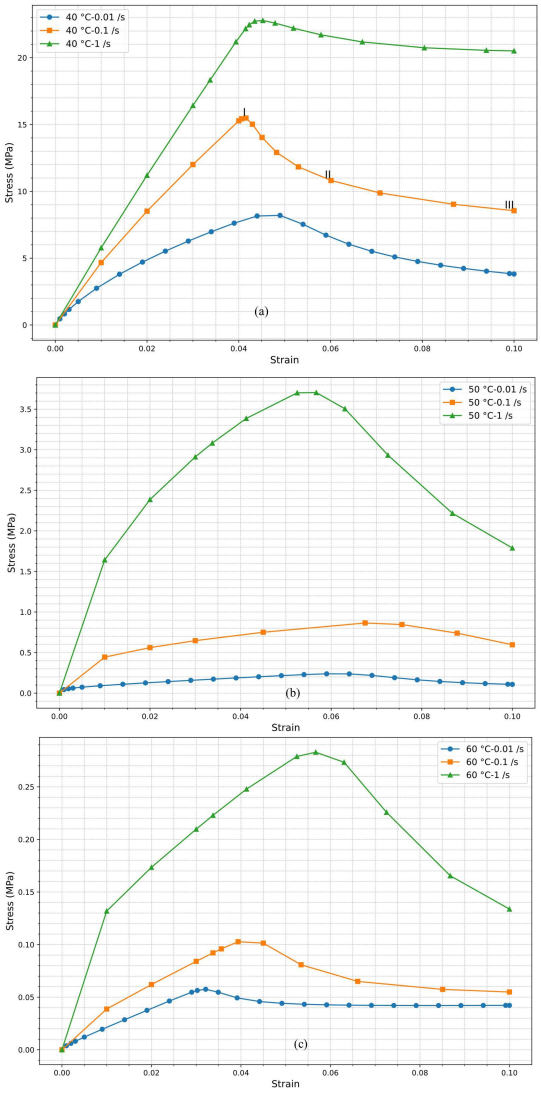

Fig. 6. Stress-strain response of holed auxetic structures at different strain rates and temperatures of (a) 40 °C, (b) 50 °C, and (c) 60 °C.

Additionally, increasing the temperature beyond the glass temperature dominates the loss modulus over the storage modulus [20]; therefore, the material becomes softer in comparison to lower temperatures. Thus, the critical strain occurs at lower deformations as the material's resistance decreases.

Energy harvesting involves capturing and converting energy into electrical power. Deformation energy can serve as a viable source for harvesting if it can be stored and recovered when needed. However, plastic deformation energy is generally unsuitable for energy harvesting devices, as it is absorbed by the material and dissipated as heat. While elastic energy in soft materials can be recovered, it is not suitable for energy harvesting since the load must remain on the material; removing the load causes the material to revert to its undeformed shape. In contrast, shape memory materials can store energy during high-temperature deformation (above the glass transition temperature), retain this energy and deformation upon cooling, and ultimately convert it into electrical energy when reheated. The area under each stress-strain curve in Fig. 6 was computed using the trapezoidal rule from the Python trapezoid function of the SciPy library, and the results are presented in Fig. 9. It is evident that by increasing the loading rate, the absorbed energy increases from 0.53 J/cm^3 to 1.72 J/cm^3 while an increase in temperature leads to a reduction in stored energy.

As demonstrated, shape memory materials can respond to both heat and loading rate stimuli. This characteristic can be leveraged to adjust the Poisson's ratio in auxetic structures by applying these stimuli, thereby altering the cell opening. This behavior has potential applications in drug delivery systems or soft actuators. The Poisson's ratio (υ) is defined by Eq. (2), where ε_t represents the transverse strain and ε_a corresponds to the axial strain:

$$\upsilon = -\frac{\varepsilon_t}{\varepsilon_a} \tag{2}$$

It is worth mentioning that deformation is not uniform throughout the specimen, which results in a non-constant Poisson's ratio across the sample. Therefore, the Poisson's ratio was determined at the center of the samples, where the minimum Poisson's ratio was generally observed. The results of the Poisson's ratio at different temperatures and strain rates are presented in Fig. 10. It can be concluded that during the initial stages of deformation, the Poisson's ratio is positive (approximately 0.4), indicating non-auxetic behavior. However, after pattern transformation, the Poisson's ratio becomes zero or negative. This is an intriguing aspect of engineering design, where shape memory polymers can be pre-programmed to achieve a desired Poisson's ratio for subsequent use. For example, in applications such as shape memory stents, a near-zero

Poisson's ratio is desirable, whereas in sensors, actuators, and implants, a negative Poisson's ratio can provide optimal performance. Looking forward, the ability to tune the Poisson's ratio through deformation and external stimuli could open new avenues for designing advanced engineering components.

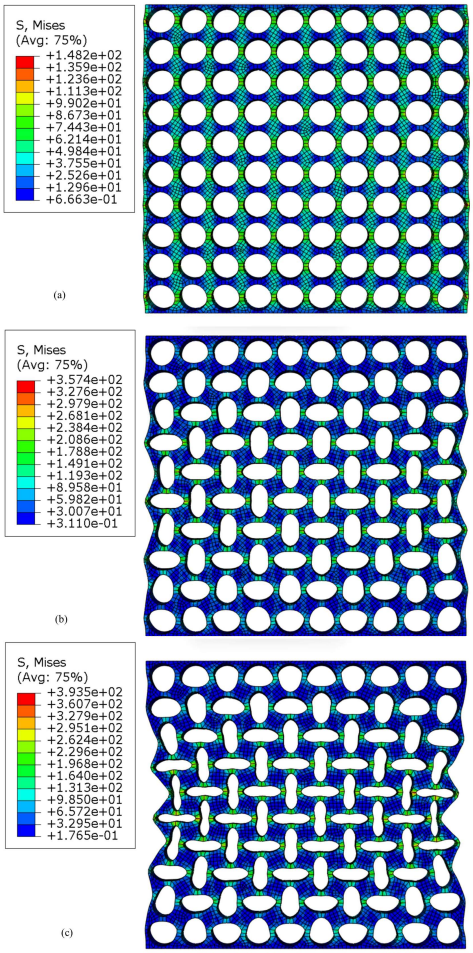

Fig. 7. Deformed geometries of the circular-holed auxetic structure at points: (a) I, (b) II, and (c) III in Fig. 6 (a).

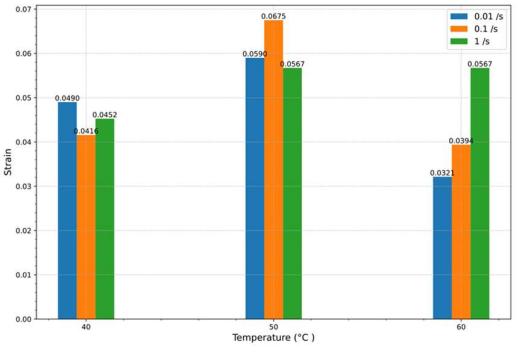

Fig. 8. Critical strain versus temperature at different strain rates.

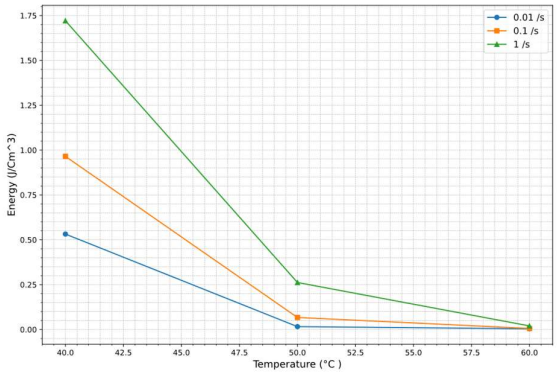

Fig. 9. Stored energy during shape memory programming versus temperature at different strain rates.

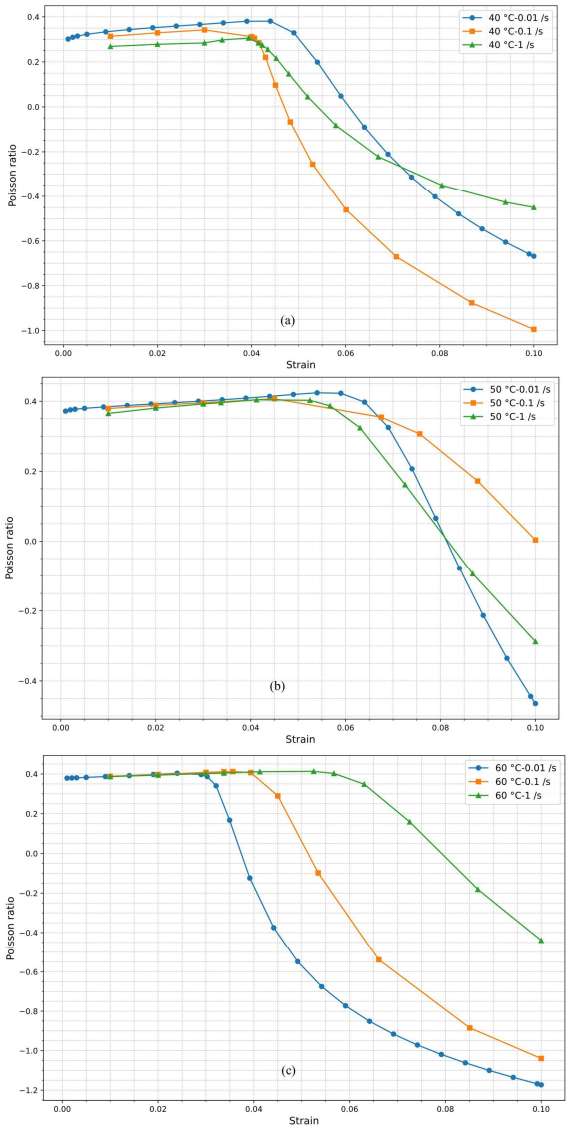

Fig. 10. Poisson's ratio versus axial strain at (a) 40 °C, (b) 50 °C, and (c) 60 °C.

To understand the effect of time and temperature on the variation of Poisson's ratio, the relaxation behavior of shape memory materials, particularly near the glass transition temperature, must be considered. As shown in Table 2, increasing the strain rate decreases the loading time during compression (post-buckling) analyses. When the loading time is reduced, the material has insufficient time to relax, whereas, at lower strain rates, the loading time is sufficient for relaxation. Relaxation simulations were conducted under the conditions outlined in Table 3 at various temperatures, and the results are presented in Fig. 11.

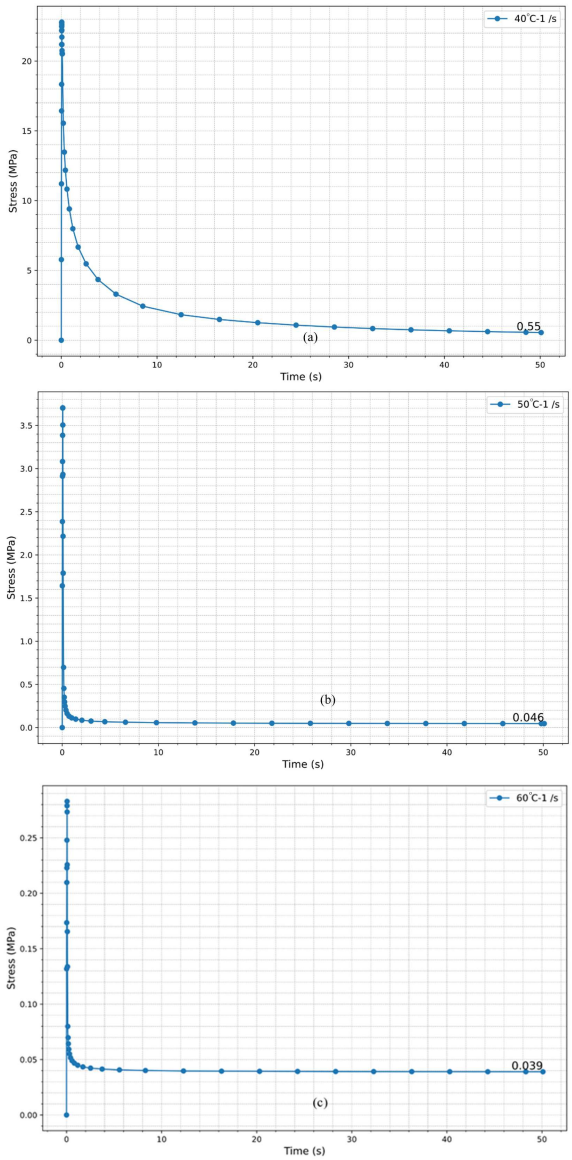

Fig. 11. Relaxation simulation results at (a) 40 °C, (b) 50 °C, and (c) 60 °C.

It should be noted that, in both relaxation simulations and experiments, loading must be applied immediately to prevent relaxation during the loading phase of the test. Therefore, in the relaxation simulations, a minimum time of 0.1 s was used, corresponding to a strain rate of 1 /s.

From Fig. 11, it is evident that an increase in temperature leads to a reduction in both peak and equilibrium stress. Figs. 11(b) and 11(c) show that at temperatures above the glass transition temperature (T_g), the material exhibits significant relaxation over short periods. This indicates that deformation and relaxation mechanisms are active at low strain rates during compressive loading. Consequently, in Fig. 10(a), sufficient time is available for stress relaxation at a low strain rate of 0.01 /s, resulting in reduced transverse deformation under the applied load. Conversely, at a strain rate of 1 /s, there is insufficient time for relaxation in any part of the sample, leading to more uniform transverse deformation, producing less transverse strain and, thus, a lower Poisson's ratio. These observations are further illustrated in different sections of Fig. 12. Fig. 12(b) shows that reduced relaxation leads to more significant transverse displacement, thereby increasing the Poisson's ratio. Minimal relaxation (corresponding to higher stress) results in more uniform deformation within the sample but with reduced transverse displacement or strain.

While this research focuses on the mechanical behavior of cellular auxetic structures, future studies could explore the intriguing mechanical properties of other auxetic types, such as rigid body rotation-based, chiral, and re-entrant auxetic structures.

4. Conclusion

This study investigated the post-buckling behavior of an open cellular structure with circular holes across different temperatures and strain rates. Relaxation simulations were conducted to deepen the understanding of auxetic behavior. The Neo-Hookean hyperelastic model was employed to describe the elastic behavior of the epoxy shape memory polymer, while a viscoelastic model using the Prony series accounted for the

material's memory effect. Geometrical imperfections from buckling analysis were introduced into the non-linear analysis of auxetic structures. The results indicated that imperfections significantly influence the loading response and deformation modes of these structures. During the initial buckling phase, variations in the imperfection factor led to different deformation modes, ranging from local buckling to more homogeneous deformation. The final deformed geometry at large strains remained independent of the imperfection factor, as the geometry densified. Additionally, non-homogeneous deformation of auxetic structures was observed when periodic boundary conditions were applied.

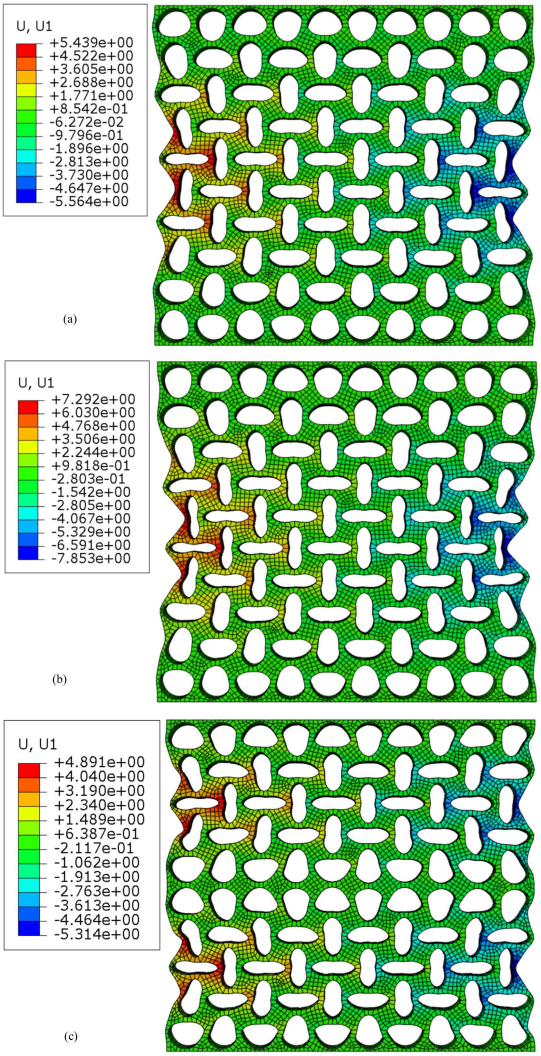

Fig. 12. Final deformed geometry at 40 °C at (a) 0.01 /s, (b) 0.1 /s, and (c) 1 /s.

The study also revealed that the critical strain increases with temperature up to the glass transition temperature, then decreases with further increase in temperature. Furthermore, the stored energy decreased with temperature, as the loss modulus increased.

Acknowledgments

The authors express their gratitude to the research board of K. N. Toosi University of Technology for their financial support and provision of research facilities utilized in this study.

Conflict of interest

The authors declare that there is no conflict of interest in this research.

Funding

The authors declare that no funds, grants, or other support were received during the preparation of this manuscript.

5. References

[1] Critchley, R., Smy, V., Corni, I., Wharton, J. A., Walsh, F. C., Wood, R. J., & Stokes, K. R. (2020). Experimental and computation assessment of thermomechanical effects during auxetic foam fabrication. *Scientific Reports*, *10*(1), 18301. https://doi.org/10.1038/s41598-020-75298-w

[2] Hu, J., He, Y., Lei, J., & Liu, Z. (2013). Novel mechanical behavior of periodic structure with the pattern transformation. *Theoretical and Applied Mechanics Letters, 3*(5), 054007. https://doi.org/10.1063/2.1305407

[3] He, Y., Guo, S., Liu, Z., & Liew, K. M. (2015). Pattern transformation of thermo-responsive shape memory polymer periodic cellular structures. *International Journal of Solids and Structures, 71*, 194-205. https://doi.org/10.1016/j.ijsolstr.2015.06.022

[4] Bertoldi, K., Reis, P. M., Willshaw, S., & Mullin, T. (2010). Negative Poisson's ratio behavior induced by an elastic instability. *Advanced Materials*, *22*(3), 361-366. https://doi.org/10.1002/adma.200901956

[5] Forte, A. E., Melancon, D., Zanati, M., De Giorgi, M., & Bertoldi, K. (2023). Chiral mechanical metamaterials for tunable optical transmittance. *Advanced Functional Materials, 33*(20), 2214897. https://doi.org/10.1002/adfm.202214897

[6] Duncan, O., Foster, L., Allen, T., & Alderson, A. (2023). Effect of Poisson's ratio on the indentation of open cell

foam. *European Journal of Mechanics-A/Solids*, 99, 104922. https://doi.org/10.1016/j.euromechsol.2023.104922

[7] He, P., Wang, S., Zhang, M., Sang, L., Tong, L., & Hou, W. (2024). Compression performance of 3D-printed thermoplastic auxetic structures. *Thin-Walled Structures, 197*, 111558. https://doi.org/10.1016/j.tws.2024.111558

[8] Gatt, R., Wood, M. V., Gatt, A., Zarb, F., Formosa, C., Azzopardi, K. M., Casha, A., Agius, T. P., Schembri-Wismayer, P., Attard, L., & Chockalingam, N. (2015). Negative Poisson's ratios in tendons: An unexpected mechanical response. *Acta Biomaterialia, 24*, 201-208. https://doi.org/10.1016/j.actbio.2015.06.018

[9] Eghbali, P., Younesian, D., Moayedizadeh, A., & Ranjbar, M. (2020). Study in circular auxetic structures for efficiency enhancement in piezoelectric vibration energy harvesting. *Scientific Reports, 10*(1), 16338. https://doi.org/10.1038/s41598-020-73425-1

[10] Peng, C., Tran, P., & Mouritz, A. P. (2022). Compression and buckling analysis of 3D printed carbon fibre-reinforced polymer cellular composite structures. *Composite Structures, 300*, 116167. https://doi.org/10.1016/j.compstruct.2022.116167

[11] Johnson, C. G., Jain, U., Hazel, A. L., Pihler-Puzović, D., & Mullin, T. (2017). On the buckling of an elastic holey column. *Proceedings of the Royal Society A: Mathematical, Physical and Engineering Sciences, 473*(2207), 20170477. https://doi.org/10.1098/rspa.2017.0477

[12] Bertoldi, K., Boyce, M. C., Deschanel, S., Prange, S., & Mullin, T. (2008). Mechanics of deformation-triggered pattern transformations and superelastic behavior in periodic elastomeric structures. *Journal of the Mechanics and Physics of Solids, 56*(8), 2642-2668. https://doi.org/10.1016/j.jmps.2008.03.006

[13] Talezadehlari, A., & Rahimi, G. H. (2017). The effect of geometrical imperfection on the axial buckling of unstiffened and stiffened composite cylinders with and without cutout. *Modares Mechanical Engineering, 17*(7), 245-256. https://doi.org/20.1001.1.10275940.1396.17.7.33.5

[14] Dassault Systèmes. (2012). *Abaqus/CAE user's manual (Version 6.12)*. Dassault Systèmes.

[15] Tafreshi, A., & Bailey, C. G. (2007). Instability of imperfect composite cylindrical shells under combined loading. *Composite Structures, 80*(1), 49-64. https://doi.org/10.1016/j.compstruct.2006.02.031

[16] Su, P., Yang, Y., & Song, Y. (2015). Corneal hyper-viscoelastic model: derivations, experiments, and simulations. *Acta of Bioengineering and Biomechanics, 17*(2), 73-84. https://doi.org/10.5277/ABB-00142-2014-03

[17] Li, C., & Lua, J. (2009). A hyper-viscoelastic constitutive model for polyurea. *Materials Letters, 63*(11), 877-880. https://doi.org/10.1016/j.matlet.2009.01.055

[18] Narooei, K., & Arman, M. (2018). Generalization of exponential based hyperelastic to hyper-viscoelastic model for investigation of mechanical behavior of rate dependent materials. *Journal of the Mechanical Behavior of Biomedical Materials, 79*, 104-113. https://doi.org/10.1016/j.jmbbm.2017.12.019

[19] Janbaz, S., Narooei, K., Van Manen, T., & Zadpoor, A. (2020). Strain rate–dependent mechanical metamaterials. *Science Advances, 6*(25), eaba0616. https://doi.org/10.1126/sciadv.aba0616

[20] Diani, J., Gilormini, P., Frédy, C., & Rousseau, I. (2012). Predicting thermal shape memory of crosslinked polymer networks from linear viscoelasticity. *International Journal of Solids and Structures, 49*(5), 793-799. https://doi.org/10.1016/j.ijsolstr.2011.11.019

[21] Hu, J., Zhou, Y., Liu, Z., & Ng, T. Y. (2017). Pattern switching in soft cellular structures and hydrogel-elastomer composite materials under compression. *Polymers, 9*(6), 229. https://doi.org/10.3390/polym9060229

[22] Taylor, M., Francesconi, L., Baldi, A., Liang, X., & Aymerich, F. (2019). A novel auxetic structure with enhanced impact performance by means of periodic tessellation with variable Poisson's ratio. In *Dynamic Behavior of Materials, Volume 1: Proceedings of the 2018 Annual Conference on Experimental and Applied Mechanics* (pp. 211-218). Springer International Publishing.

[23] Liang, X. (2018). *Design of metamaterials with graduating Poisson's ratio through periodic void patterns* [Master's Theses, Santa Clara University]. https://scholarcommons.scu.edu/mech_mstr/20

[24] Javid, F., Liu, J., Shim, J., Weaver, J. C., Shanian, A., & Bertoldi, K. (2016). Mechanics of instability-induced pattern transformations in elastomeric porous cylinders. *Journal of the Mechanics and Physics of Solids, 96*, 1-17. https://doi.org/10.1016/j.jmps.2016.06.015

[25] Overvelde, J. T. B., Shan, S., & Bertoldi, K. (2012). Compaction through buckling in 2D periodic, soft and porous structures: effect of pore shape. *Advanced Materials, 24*(17), 2337-2342. https://doi.org/10.1002/adma.201104395

[26] Box, F., Johnson, C. G., & Pihler-Puzović, D. (2020). Hard auxetic metamaterials. *Extreme Mechanics Letters, 40*, 100980. https://doi.org/10.1016/j.eml.2020.100980

[27] Pence, T. J., & Gou, K. (2015). On compressible versions of the incompressible Neo-Hookean material. *Mathematics and Mechanics of Solids, 20*(2), 157-182. https://doi.org/10.1177/1081286514544258

[28] Ghorbanoghli, A., & Narooei, K. (2019). A new hyper-viscoelastic model for investigating rate dependent mechanical behavior of dual cross link self-healing hydrogel. *International Journal of Mechanical Sciences, 159*, 278-286. https://doi.org/10.1016/j.ijmecsci.2019.06.019

[29] Hiemenz, P. C., & Lodge, T. P. (2007). *Polymer chemistry*. CRC press.

[30] Sadeghi, F., Baniassadi, M., Shahidi, A., & Baghani, M. (2023). TPMS metamaterial structures based on shape memory polymers: Mechanical, thermal and thermomechanical assessment. *Journal of Materials Research and Technology, 23*, 3726-3743. https://doi.org/10.1016/j.jmrt.2023.02.014